

Afferent Influences on Brain Stem Auditory Nuclei of the Chicken: Time Course and Specificity of Dendritic Atrophy Following Deafferentation

JEFFREY S. DEITCH AND EDWIN W. RUBEL

Departments of Otolaryngology and Physiology, and Neuroscience Program, University
of Virginia Medical Center, Charlottesville, Virginia 22908

ABSTRACT

The time course and specificity of the changes in dendritic morphology following deafferentation were examined in nucleus laminaris of young chickens. The dendrites of nucleus laminaris neurons are segregated into dorsal and ventral domains, which are innervated separately from the ipsilateral and contralateral nucleus magnocellularis, respectively. Transection of the crossed dorsal cochlear tract deafferents the ventral dendrites of nucleus laminaris bilaterally without interrupting the matching input to the dorsal dendrites.

In 10-day-old chicks, atrophy of the ventral dendrites began immediately after transecting the tract; the ventral dendrites were 10% shorter by 1 hour and 16% shorter by 2 hours after deafferentation. The length of the ventral dendrites progressively decreased over the next 2 weeks, resulting in at least a 60% loss of ventral dendrite 16 days after surgery. The dorsal dendrites of the same cells, whose afferents remained intact, did not change in length during the time course of this study. However, 16 days after the lesion, spines appeared on the normally smooth dorsal and ventral dendrites. The time course of dendritic atrophy and its restriction to the deafferented postsynaptic surface are related to possible mechanisms by which afferents regulate and maintain their target neurons.

Key words: plasticity, sensory systems, Golgi, morphometry

Understanding of the influence that afferent axons have on the normal development and maintenance of neuronal structure has been advanced greatly by observing neurons after removing all or part of their input. There is now substantial evidence that intact and functioning afferent axons play a major role in regulating the morphology (Valverde, '68; Murphey et al., '75; Benes et al., '77; Caceres and Steward, '83), metabolism (Kupfer and Downer, '67; Lippe et al., '80; Durham, '82; Durham and Woolsey, '84; Meyer and Edwards, '82), and organization (Ruiz-Marcos and Valverde, '70; Parks, '79, '81; Rubel et al., '81) of their postsynaptic cells (see reviews by Cowan, '70; and Globus, '75). Most of these studies emphasized the long-term adjustments that the postsynaptic cell makes in the absence of a particular input. However, it is also of interest to determine the short-term responses to deafferentation. Information on the time course and localization of the postsynaptic reaction to deafferentation is necessary in order to eventually spec-

ify the cellular chain of events relating presynaptic activity and integrity to the structure and function of postsynaptic neurons.

The dendrites of a neuron provide a logical place to investigate the events underlying afferent regulation of neuronal structure. Dendrites generally have stereotypic properties, and different classes of afferents often are limited to specific sites on the postsynaptic surface. Indeed, removal of afferent innervation results in a variety of changes in gross dendritic morphology (Jones and Thomas,

Accepted April 19, 1984.

Portions of this research have been presented elsewhere (Rubel and Smith, '81; Deitch and Rubel, '82).

Address reprint requests to Dr. E. W. Rubel, Dept. of Otolaryngology, Box 430, University of Virginia Medical Center, Charlottesville, VA 22908.

'62; Liu and Liu, '71; Murphey et al., '75; Benes et al., '77; Bernstein and Standler, '83) and ultrastructure of the postsynaptic specializations (White and Westrum, '64; Gentschev and Sotelo, '73; Pinching and Powell, '71; Wisniewski et al., '72; Gulley et al., '77). The present study examines the temporal and spatial relationships between the alterations in the pattern of innervation and the changes observed in the postsynaptic cell within the brain stem auditory pathways of the chicken.

Nucleus laminaris (NL), an avian third-order auditory nucleus, is a homogeneous monolayer of cell bodies in the dorsal medulla whose dendrites are spatially segregated into dorsal and ventral domains. The major inputs to NL come from the ipsilateral and contralateral second-order auditory nuclei, *n. magnocellularis* (NM, Ramón y Cajal, '08; Boord, '69; Parks and Rubel, '75; Parks et al., '83). Afferents from NM bifurcate, sending one collateral to the dorsal neuropil of the ipsilateral NL and the other collateral to the ventral neuropil of the contralateral NL via the crossed dorsal cochlear tract (XDCT). This arrangement results in a spatially segregated, binaural, excitatory input to each NL cell (Rubel and Parks, '75; Hackett et al., '82; Young and Rubel, '83).

Studies of the morphology and cytoarchitecture of NL revealed that the length and number of the dendrites vary systematically as a function of the rostrocaudal and mediolateral position of the cell within the nucleus, corresponding to the tonotopic organization of NL (Smith and Rubel, '79; Smith, '81). A consequence of this organization is that the dendritic length and the number of primary dendrites on each side of normal NL cells can be predicted from the location of the cell within the nucleus and compared with measurements obtained following various manipulations. Furthermore, since the dorsal and ventral dendrites of each NL cell are normally of equivalent size (Smith and Rubel, '79; Smith, '81), one dendritic surface of a neuron can be used to represent the control condition when manipulations are performed that are limited to the other dendritic surface (Benes et al., '77). We have taken advantage of one such manipulation; transection of the XDCT removes the major input to the ventral dendrites, while leaving intact the input to the dorsal dendrites of the NL neurons (Benes et al., '77; Rubel et al., '81). In the present study, a detailed analysis was made of the time course and specificity of changes in dendritic size following this manipulation. The results demonstrate that the morphological changes in NL cells following partial deafferentation begin immediately, are localized to the deafferented surface, and occur simultaneously throughout the nucleus.

MATERIALS AND METHODS

Approximately 150 chickens of either the Hubbard or Ross Arbor Acres strain were used for qualitative and quantitative analyses. All subjects were incubated and hatched in the laboratory and raised in heated, communal brooders with free access to food and water.

Surgery and histology

Nine- to 12-day-old chickens were anesthetized with 1.5 cc/kg body weight of Chloropent (Fort Dodge Labs) potentiated by 80 mg/kg body weight of ketamine HCl (Ketalar, Parke-Davis) and placed in a head holder. The neck muscles were exposed, injected with 0.1 cc of 2% Xylocaine, and resected to expose the dura covering the cerebellomedullary

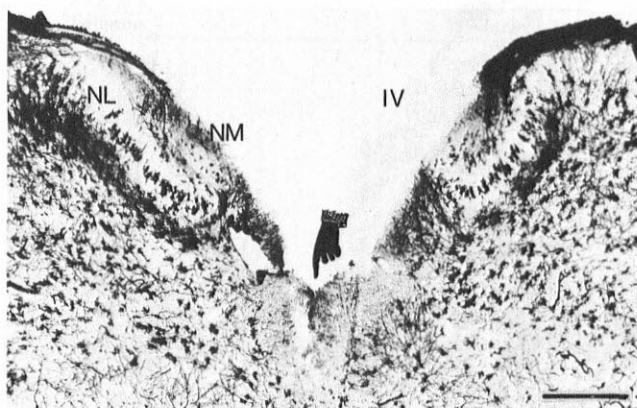


Fig. 1. Low-power micrograph of a 120- μ m-thick coronal section through a chick brain stem 8 hours after surgery, showing nucleus magnocellularis (NM), nucleus laminaris (NL), and the crossed dorsal cochlear tract transection (indicated by the pointer). Note the clear zone surrounding the cells of NL, which consists of a shell of NM myelinated axons. IV, fourth ventricle. Golgi-Kopsch stain. Bar = 500 μ m.

cistern. An ophthalmic knife was inserted through the dura and the fourth ventricle and into the brain stem so as to transect the crossed dorsal cochlear tract at the midline (Fig. 1). The wound was packed with gelfoam and the skin sutured. The control animals were unoperated and sham-operated chickens, the latter having had a knife inserted into the fourth ventricle without injuring the NM axons.

After survival times of 1, 2, 4, 8, or 12 hours, or 1, 2, 4, 8, or 16 days, the chickens were anesthetized with Chloropent and perfused transcardially with Golgi-Kopsch fixative, and the brains were processed according to a modification of the del Rio-Hortega Golgi-Kopsch method (Stensaas, '67). The brains were either dehydrated in ethanol, embedded in nitrocellulose, and sectioned on a sliding microtome, or sectioned without embedding, using an Oxford vibratome, and then dehydrated. The vibratome-sectioned tissue yielded the best results in terms of clarity and impregnation density. In both procedures, the serial 100–200- μ m coronal sections were cleared in cedarwood oil or terpineol and mounted in either Permount or Lipshaw Mounting Medium.

Transection of the XDCT resulted in a dramatic decrease in the number of NL cells stained by the Golgi impregnation procedure used in previous studies (Smith and Rubel, '79; Smith, '81). The failure to impregnate deafferented cells with a Golgi method is a common occurrence (e.g., see Pinching and Powell, '71; and Smith, '74). Decreasing the infiltration time to 60 hours for fixative and 36 hours for silver nitrate (from 72 hours and 48 hours, respectively) resulted in full impregnation of NL cells equal in clarity and number to that attained with the longer procedure on normal chicks.

The crossed dorsal cochlear tract consists of a sheet of tightly packed, heavily myelinated axons that are quite visible in Golgi-impregnated sections under phase-contrast or darkfield illumination. This allowed us to directly assess the completeness of the transection and discard those brains in which the tract was not completely severed throughout its rostrocaudal extent.

TABLE 1. Number of cells used for quantitative analyses

Survival time (# of animals)	# of cells sampled
Controls:	77
Sham-operated (2)	
Unoperated (4)	
1 hour (3):	52
2 hours (4):	74
4 hours (3):	56
8 hours (3):	73
12 hours (4):	57
1 day (2):	64
2 days (4):	25
4 days (2):	35
8 days (3):	45
16 days (2):	34

Additional subjects with survival times of 1, 2, 8, 12, 24, and 48 hours after XDCT transection were prepared in order to examine the glial reaction to the lesion in Nissl-stained tissue. Two chickens from each of these survival times were perfused transcardially with phosphate-buffered 10% formalin. The brains were embedded in paraffin and every fourth 10- μm coronal section through the brain stem was stained with thionin.

Quantification of dendrites

In all, 592 cells from 36 animals were used for quantitative measurements (see Table 1). Cells were selected randomly, with the constraint that the sample contain representative cells from all areas of the nucleus in order to detect any regional variations in the response to deafferentation. A cell was drawn if it met the criteria defined by Smith and Rubel ('79): in brief, the cell must belong to NL, the entire section must appear homogeneously impregnated, all the dendrites of the cell must be contained within a single section, and the dorsal and ventral dendrites must be distinguishable and traceable throughout their entire lengths. Cells were drawn under camera lucida using a $\times 100$ Neofluar objective (n.a. = 1.3) at a final magnification of $\times 1,350$ or $\times 2,000$.

Two types of drawings were made. For all cells, a line was drawn through the center of each dendritic process for its entire length, giving a stick-figure representation of the cell's dendrites. Although these two-dimensional drawings foreshorten the nonplanar NL dendrites, the splay of the dendrites is minor in both control and experimental animals, such that the measured lengths are proportional to the actual lengths (Smith and Rubel, '79). Dorsal and ventral dendritic lengths were measured from the stick-figure drawings using a digitizing tablet with a Zeiss Videoplan image analysis system. In addition, drawings were made of the longitudinal cross-sectional area of the dendrites of 27 cells by outlining them in silhouette. The dorsal and ventral dendritic areas were computed from these silhouette drawings and correlated with the dendritic lengths obtained from the stick-figure drawings (Fig. 2). Repeated stick-figure drawings of some of the cells by camera lucida produced lengths that differed at most by 20 μm (2–10%), and measurements using the Videoplan were also highly reproducible (within 5 μm).

Data analyses

The dendritic length and the number of primary dendrites of a normal NL cell are predictable from the position

of the neuron with NL (Smith and Rubel, '79). Any change in the length or number of the dendrites after deafferentation will appear as a reliable deviation from these predicted values. Therefore, each cell in this study was assigned a set of coordinates describing its position in a planar projection of the nucleus, i.e., the percent distance along the posterior-to-anterior extent and the lateral-to-medial extent of the nucleus (see Fig. 5A,B; Rubel and Parks, '75).

For statistical analyses of the dendritic length measurements, the nucleus was divided into eight sectors such that the cells within a given sector had dendrites of similar size and number (see Smith and Rubel, '79). The average dorsal and ventral dendritic lengths were calculated for each sector, and these means were compared across survival times by an analysis of variance. The same computations were performed on the number of primary dendrites. Cells from all animals in each group could be combined in this manner since there were no reliable differences in dendritic length and number between subjects within each group as a function of position. In a separate set of analyses, the difference between the dorsal and ventral dendritic lengths was calculated on a cell-by-cell basis. Scatterplots of these data were analyzed by regressions that compared the relative sizes of the ventral (deafferented) and the dorsal dendrites as a function of time after XDCT transection.

The data were also examined for regional variations in the effects of the XDCT lesion within the nucleus. To do this we have made use of the fact that the cells of NL are arranged tonotopically (Rubel and Parks, '75) such that the characteristic frequency of a cell (CF, the acoustic frequency

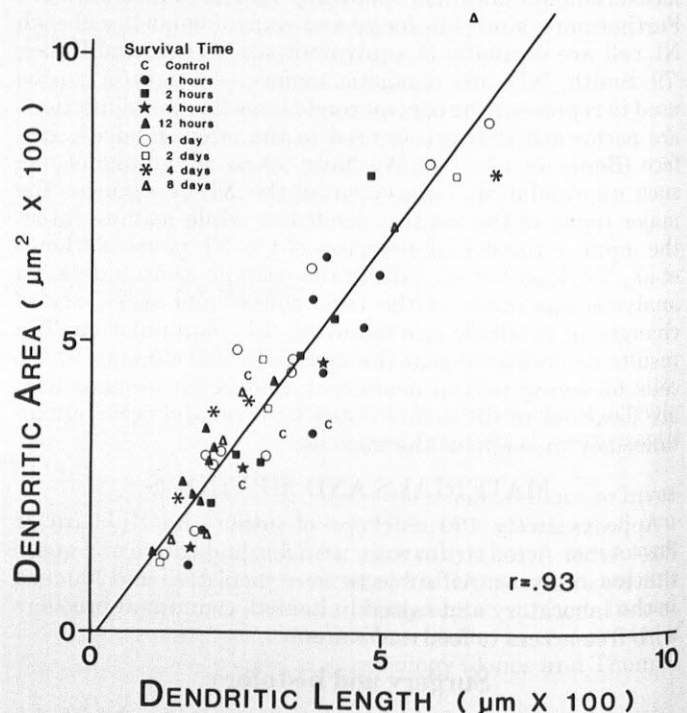


Fig. 2. Scatterplot and least-squares regression describing the relationship between the length (derived from stick-figure drawings) and the cross-sectional area (derived from silhouette drawings) of NL dendrites. Dorsal and ventral dendrites were measured separately and the data pooled. Two to five cells were drawn from normal and experimental chickens at the survival times indicated. r = Pearson product moment correlation coefficient.

to which a cell is most sensitive) increases systematically from the caudolateral to the rostromedial pole of the nucleus. This frequency axis through NL coincides with the gradient of dendritic length through NL (Fig. 5B; Smith and Rubel, '79). Since the CF can be calculated from the positional coordinates, it is a single value that estimates the position of a cell within the nucleus.¹ Therefore, we used the CF to examine the relationships between the dendritic parameters and position of the neuron within the nucleus. All statistical analyses were performed using SPSS programs on a CDC Cyber 730 computer.

RESULTS

Methodological assessment

It is not possible to unequivocally confirm the complete impregnation of cells by the Golgi method. However, there were many indications that the material used in this study accurately represented the NL cells. First, the size and dendritic form of NL cells seen in Golgi-impregnated material were comparable to a sample of NL cells observed after intracellular horseradish peroxidase injection (Hackett and Rubel, unpublished observations). Second, electron micrographic examination of the NL neuropil revealed dendritic profiles at distances from the cell body lamina that were consistent with those seen in Golgi-impregnated material. In addition, the normal material presented in this study replicates the findings of Smith and Rubel ('79) and Smith ('81), emphasizing the predictability of NL dendritic size using the Golgi technique.

The relationship between dendritic length (measured from the stick figure drawings) and dendritic area (measured from the silhouette drawings) was examined in 27 cells sampled from several survival times and sectors of the nucleus and is shown in Figure 2. Dendritic length and area were correlated ($r = 0.93$, $n = 54$) irrespective of the side of the cell, length of the dendrites, and time after deafferentation (up to 8 days). If it is assumed that the area drawn in silhouette is a function of the total surface area of the dendrites (due to the smooth, cylindrical form of the dendrites), then we can interpret any change in the measured dendritic length as being proportional to a change in the amount of available postsynaptic dendritic surface.

Qualitative results

Twenty-four hours after denervation there was noticeable dendritic asymmetry in NL, almost all of the cells now having shorter ventral dendrites than dorsal dendrites. Nevertheless, the ventral dendrites rarely displayed any signs of degeneration at least until 4 days postlesion. They were not contorted or beaded, nor did they vary in thickness, as described elsewhere (Grant, '70). At 8 and 16 days after deafferentation the ventral dendrites had severely atrophied and showed signs of degeneration. The normal anteromedial-to-posterolateral gradient of increasing dendritic length had disappeared on the ventral side of NL, but remained on the dorsal side of the nucleus. The remnant ventral dendrites were mostly short and unbranched with irregular surfaces, varying in thickness along their lengths.

The dorsal dendrites, on the other hand, appeared healthy and similar to those from the controls up to 16 days postlesion. At 16 days after denervation, spinous processes appeared on the dorsal dendrites, the soma, and on the residual ventral dendrites of neurons throughout NL. The spines appeared in rows on the dendrites and were ran-

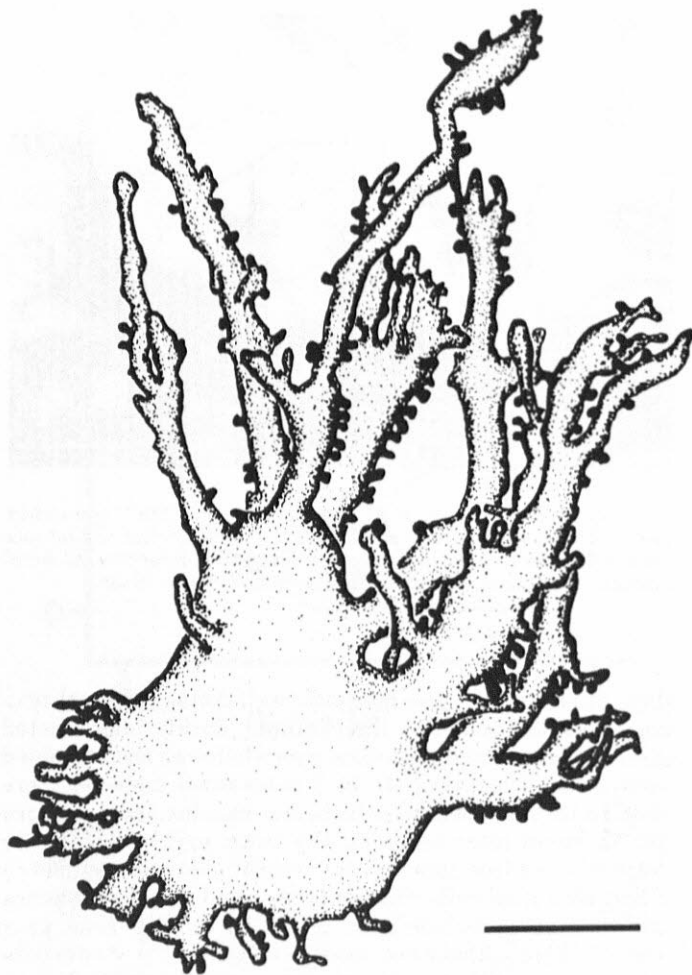


Fig. 3. Camera lucida drawing of an NL cell 16 days after XDCT transection. Note the appearance of spines, particularly on the dorsal dendrites (top), and the extensive atrophy of the ventral dendrites. (n.a. = 1.3) Bar = 10 μ m.

domly spaced on the cell body (Fig. 3). We have only observed spines on NL dendrites in normal hatchling chickens on some extreme posterolateral cells.

Satisfactory impregnation of NL cells by the Golgi-Kopsch method is normally accompanied by a lack of staining of glial somata and processes in the NL neuropil (Smith and Rubel, '79). However, beginning around 12 hours after XDCT transection, there was a noticeable increase in the number of stained glial processes extending inward from the glial zone surrounding the ventral NL neuropil. By 16

¹The positional variables, the mediolateral (L-M) and anteroposterior (P-A) percentiles, can be converted to a single number, the characteristic frequency (CF), at that cell's position by the formula

$$CF = .027 (P-A) + .014 (L-M) - .088$$

from Rubel and Parks ('75). The data were analyzed with respect to position by both the single (using the CF) and multiple (using the percentiles) linear regressions. In all cases the results of both analyses were identical.

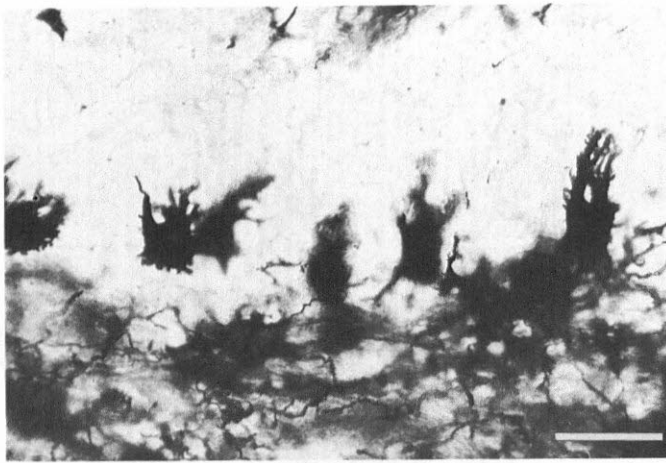


Fig. 4. Photomicrograph of NL cells 16 days after XDCT transection. Note the intrusion of glial processes into the formerly clear ventral zone (bottom) as well as the severe atrophy of the ventral dendrites. The dorsal neuropil (top) remains normal. Golgi-Kopsch stain. Bar = 50 μ m.

days after surgery, the normally well-defined ventral neuropil was dominated by intertwining, darkly impregnated glial cell bodies and processes, overwhelming the atrophied ventral dendrites (Fig. 4). In Nissl-stained material there was an invasion of glial cell bodies into the ventral neuropil 12 hours after lesioning the tract, and by 4 days the formerly cell-free zone on the ventral side was completely filled with glial cells. On the other hand, the dorsal neuropil remained a well-defined, relatively cell-free zone, as in control brains. It was not possible to determine whether the glial reaction was due to a migration of glial cell bodies, an increase in the number of glial cells, process proliferation, or any combination of these events.

Comparison of the dendrites on the deafferented and the intact sides of NL

The dorsal and ventral dendritic lengths of NL cells from the control animals were correlated ($r = .75$) and were distributed around symmetry (Fig. 5C), in agreement with previous observations (Smith and Rubel, '79; Smith, '81; Gray et al., '82). Of the cells sampled, neurons with longer dorsal dendrites were in a slight majority (58%). Transection of the XDCT resulted in a rapid upset of this dendritic balance. The relationships between the lengths of the ventral (deafferented) and dorsal (intact) dendrites from representative survival times are presented in Figures 6 and 7. Examination of the scatterplots in Figure 6 reveals a relative decrease in length of the ventral dendrites by 1 hour after XDCT transection. After 2 hours, 80% of the cells sampled had larger dorsal dendrites than ventral dendrites, and by 2 days postlesion there were no measured cells with dominant ventral dendrites. The asymmetry continued to increase over the next 2 weeks, and by 8–16 days the ventral dendrites had largely disappeared (Figs. 3, 7). There continued to be a correlation ($r > .65$) between the dorsal and ventral dendritic lengths up to 4 days postlesion. After this time the dorsal and ventral dendritic lengths showed little relationship.

Localization of changes in dendritic size

The dorsal and ventral dendritic domains were examined separately to determine whether the change in the dendritic balance reported above was due exclusively to the atrophy of the ventral dendritic processes or was confounded by a concomitant increase in the size of the dorsal dendrites. For analytic purposes we divided the nucleus into eight sectors and determined the mean dorsal and ventral dendritic lengths of neurons from each sector at each survival time. These means are presented in Figures 8A (dorsal dendrites) and 8B (ventral dendrites). The normal gradient of dendritic length in NL is illustrated in Figure 8A and B by the increasing heights of the shaded bars (the mean dendritic lengths for the control animals) from sector 1 (the anteromedial region of NL) to sector 7 (the posterolateral region of NL).² Within each set of histograms one can compare the mean dendritic lengths of one sector across the survival intervals used in this experiment. In the case of the ventral dendrites, a systematic decrease in length over time occurred within each sector. A two-way analysis of variance (survival time by sector) showed that the effect was highly reliable ($F(10,591) = 28.11$, $P < .001$). On the dorsal side of the cells there were no reliable changes in length in any sector ($F(10,591) = 1.57$, $P < .113$). This analysis demonstrates that the changes in dendritic length were exclusive to the deafferented (ventral) surface at all the times examined and suggests that the phenomenon occurs throughout the nucleus.

Quantification of the rate of dendritic atrophy

The symmetry of the two dendritic domains in normal NL cells enables us to predict the length of the dendrites on one side of the cell body from the length of the dendrites on the opposite side. Since the dorsal dendrites remained unchanged after XDCT transection, the length of the dorsal dendrites in the experimental animals becomes the best predictor of the length of the ventral dendrites prior to the lesion. Therefore, the difference between the lengths of an NL cell's dorsal and ventral dendrites estimates the amount of atrophy of the ventral dendrite following deafferentation and can be expressed as a percentage of the cell's dorsal dendritic length. Accordingly, the "percent difference" between a cell's dendritic domains is 0% if the dorsal dendritic length equals the ventral dendritic length, and is 100% if the ventral dendrites completely disappear.

The mean percent difference between the dorsal and ventral dendritic domains for the cells from the control animals in this experiment was 4%. This slight favor of dorsal dendritic length is expected from the greater number of dorsally dominant cells that were sampled (see Fig. 5C). The mean percent differences for the cells from each survival period are presented in Figure 9 as a function of time after XDCT transection. The increase in the mean percent difference was rapid in the early stages, as evident at the first survival time investigated (1 hour), and became more

²Data from sector 8 are not included in Figure 8A and B due to the small sample size obtained in this region at some of the survival intervals. For the same reason the data from sector 1 at 2 days survival time also are not presented. All cells were included in the statistical analyses, which gave the same results with or without the sector 8 values.

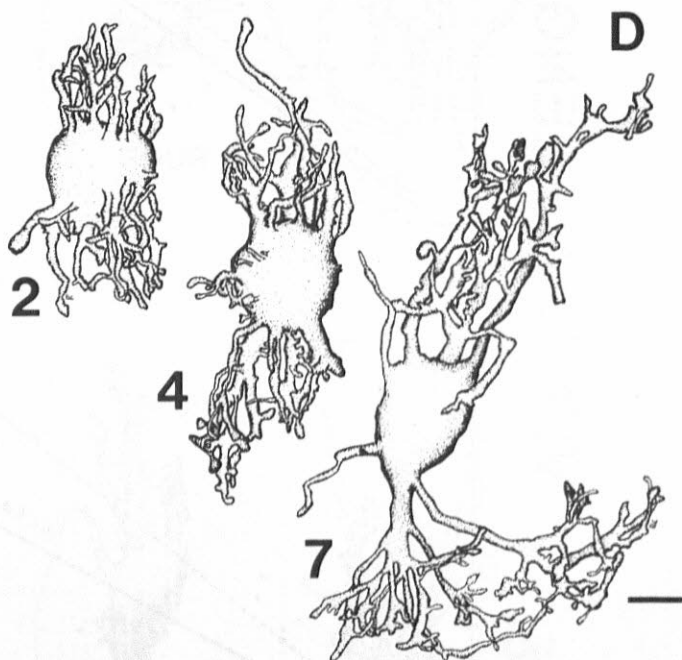
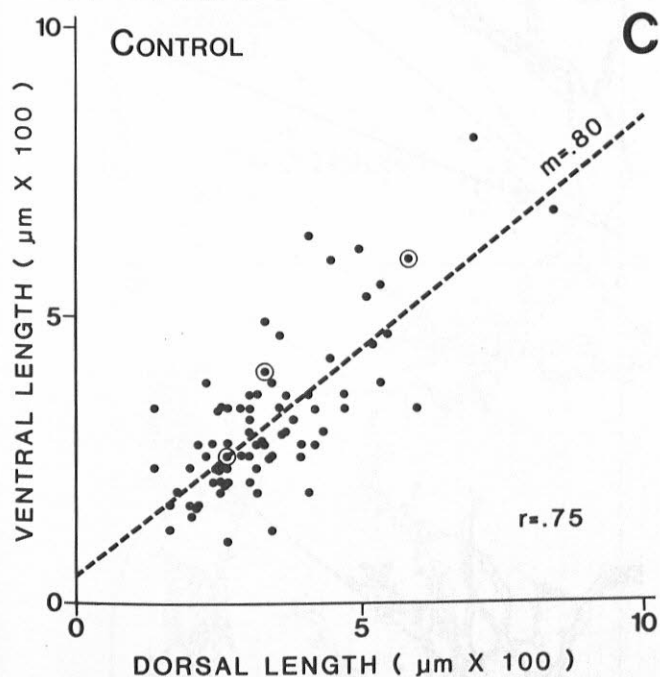
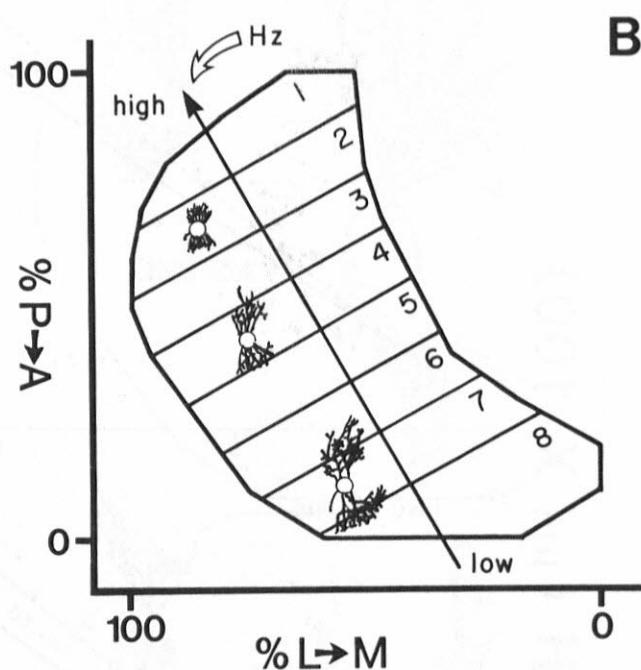
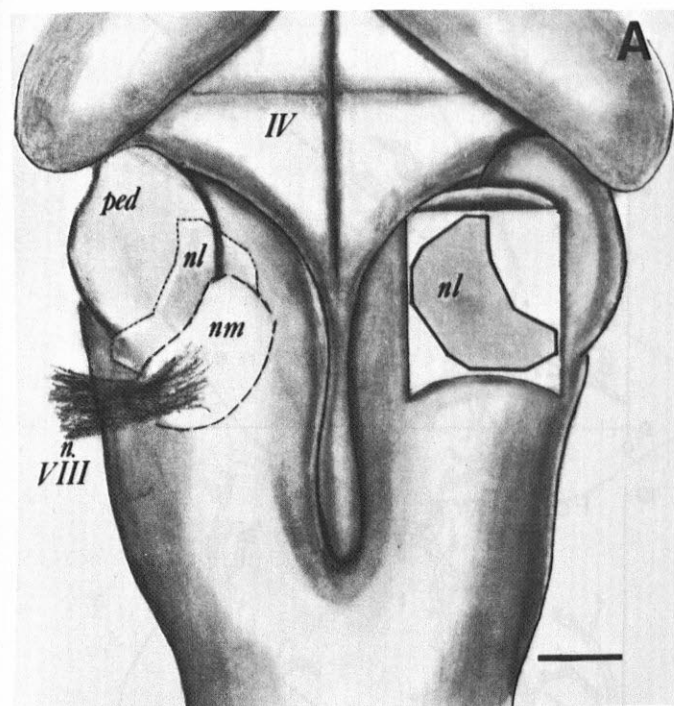


Fig. 5. A. Dorsal view of chick brain stem (cerebellum removed) showing the position of NL in the brain stem as a planar structure. nl, nucleus lamina; nm, nucleus magnocellularis; nVIII, cochlear division, eighth nerve; IV, fourth ventricle; ped, cerebellar peduncle. Bar = 1 mm. B. Planar projection of NL divided into eight sectors. The orientation of the gradient of characteristic frequency is shown. Sectors were delimited by lines drawn orthogonal to the tonotopic (frequency) axis of NL at about 400-Hz intervals. The cells within each sector have similar dendritic properties (Smith and Rubel, '79). Each cell is assigned a set of coordinates on the basis of its

percentile position on the posterior-to-anterior (% P-A) and lateral-to-medial (% L-M) axes. The positions of the cells shown in D are indicated. Hz, frequency of best response, in Hertz. C. Scatterplot and least-squares regression of the dorsal vs. ventral dendritic lengths of NL cells in normal and sham-operated chicks. The slope (m) of the regression and correlation coefficient (r) are shown ($n = 77$). The cells circled are drawn in D. D. Examples of NL cells from three sectors in NL (numbered), demonstrating the increase in dendritic length, and decrease in the number of primary dendrites from sectors 1 to 8. Normal NL dendrites do not have spines. Bar = 10 μ m.

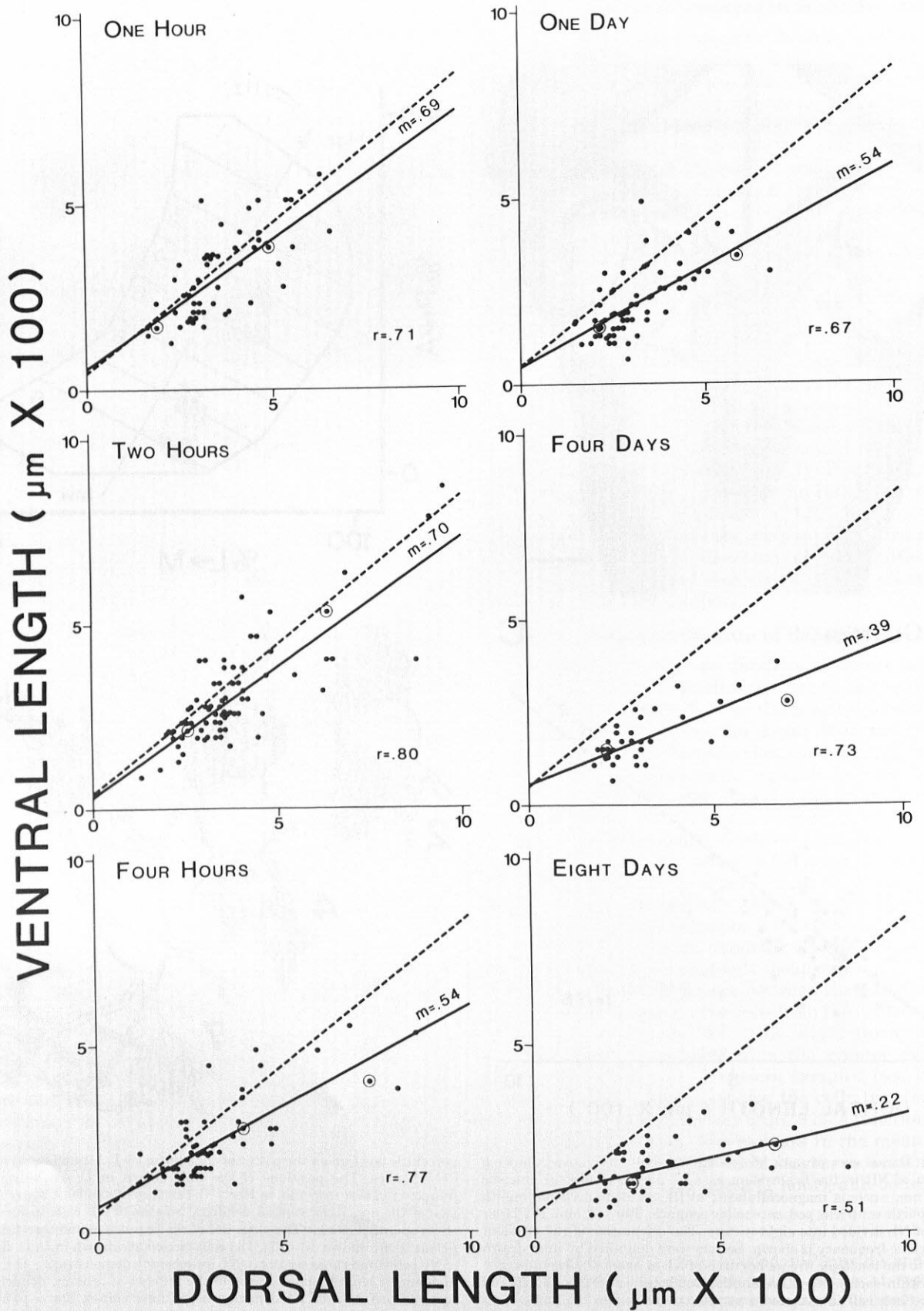


Fig. 6. The relationship between the dorsal and ventral dendritic lengths of NL cells at 1, 2, and 4 hours, and 1, 4, and 8 days after XDCT transection. The broken line represents the regression describing the population of normal cells from Figure 3. The regression for each scatterplot is shown as

a solid line. The normal symmetry of the NL dendrites begins to break down after 1 hours and continues to deteriorate, in favor of the dorsal dendrites. The slope (m) of the regression line and the correlation coefficient (r) for each group are given. Circled cells are drawn in Figure 7.

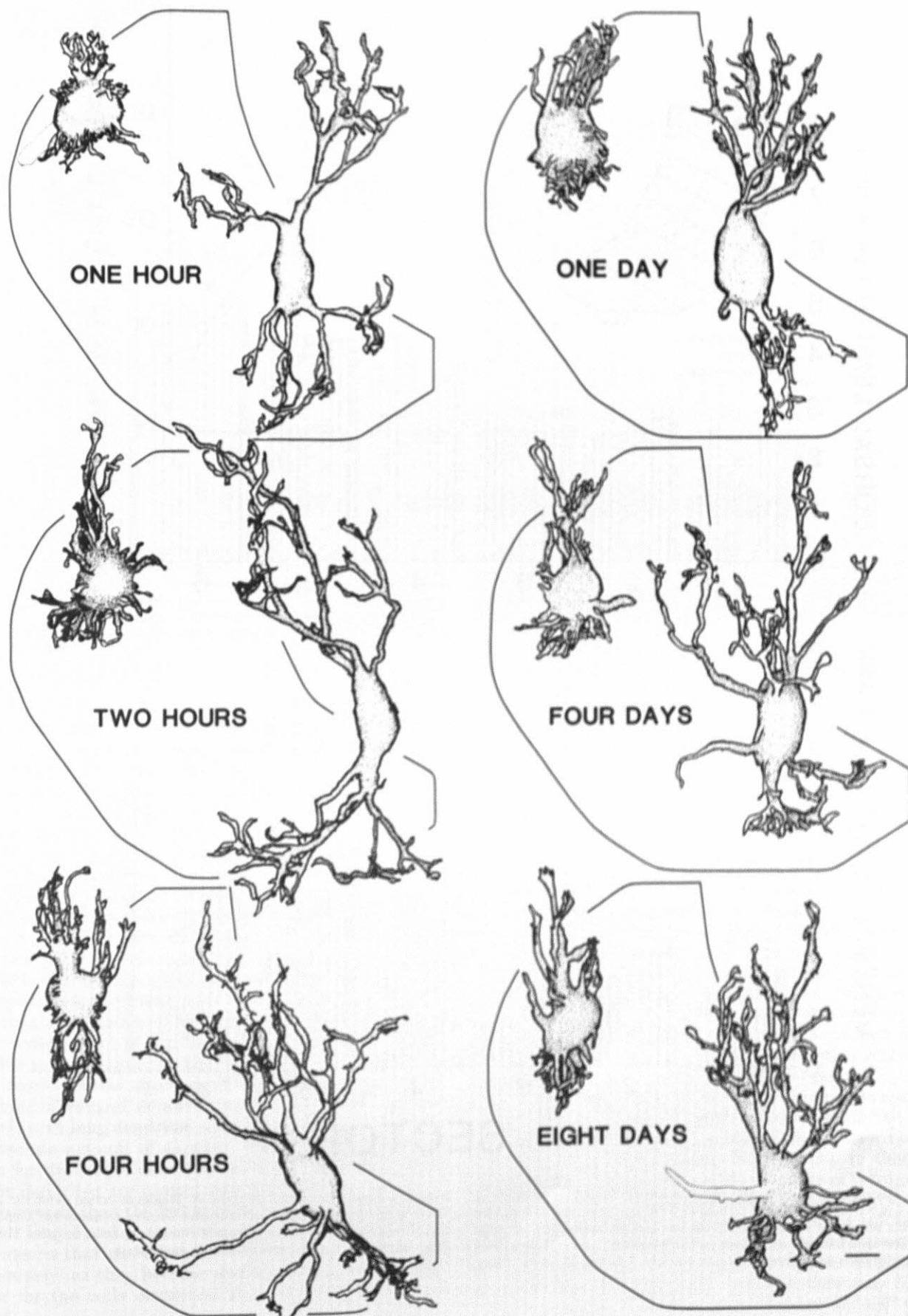


Fig. 7. Camera lucida drawings of representative cells (circled in the corresponding graph in Fig. 6) from the anteromedial and posterolateral

areas of the nucleus (circled in each graph in Fig. 6) showing the loss of symmetry of the NL cell dendrites. Bar = 10 μ m.

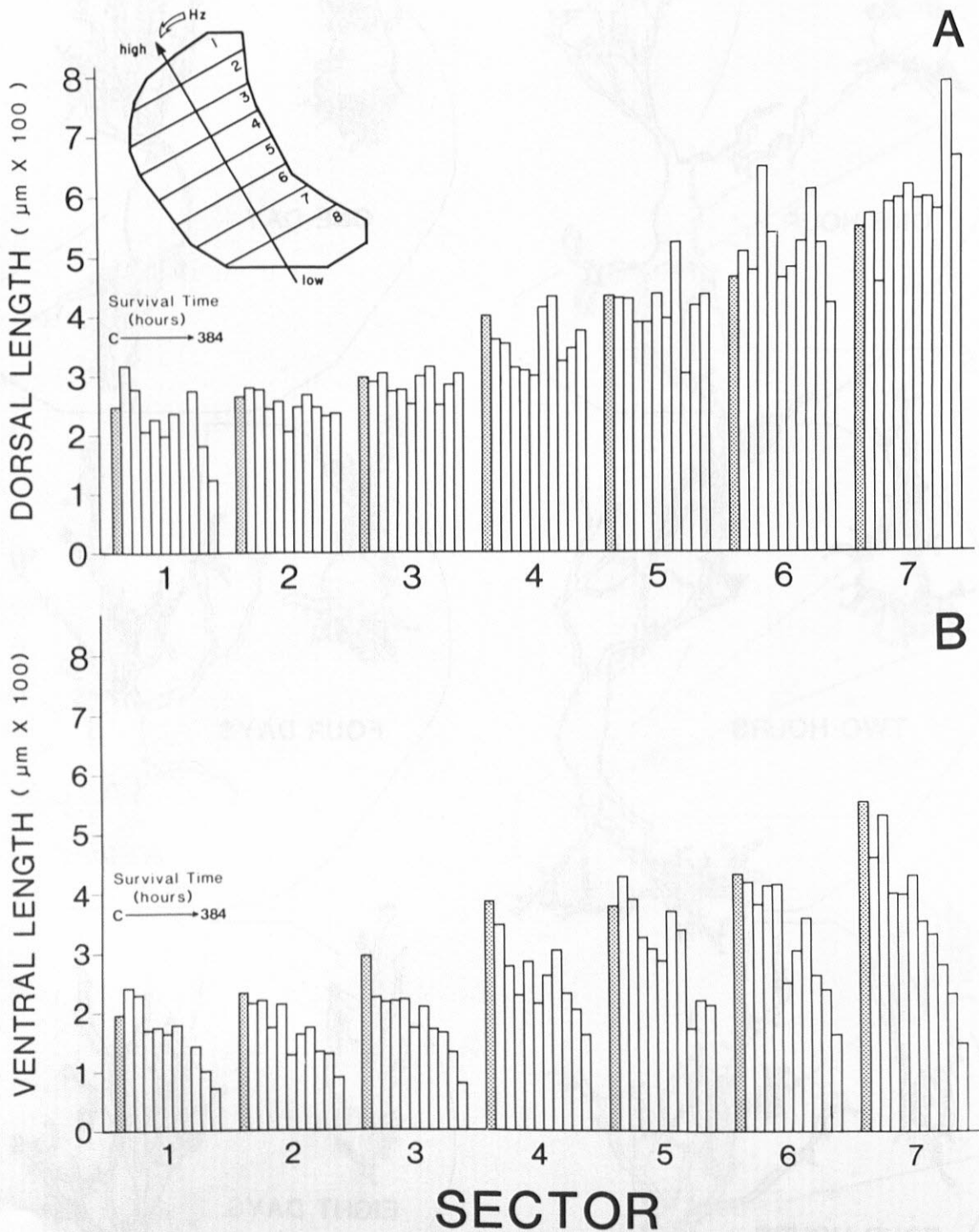


Fig. 8. Histograms showing the mean dendritic length of neurons in sectors 1-7 of NL as a function of time after XDCT transection. The shaded bar in each set is the mean value from the control and sham operated animals. The open bars are the values for the following survival times (from left to right in each set): 1 hour, 2 hours, 4 hours, 8 hours, 12 hours, 1 day,

2 days, 4 days, 8 days, and 16 days. A. Means of dorsal dendritic lengths. There is no consistent effect of time after surgery on dendritic length in the dorsal neuropil (see text). B. Means of ventral dendritic lengths. The loss of dendritic length with time is evident in each sector.

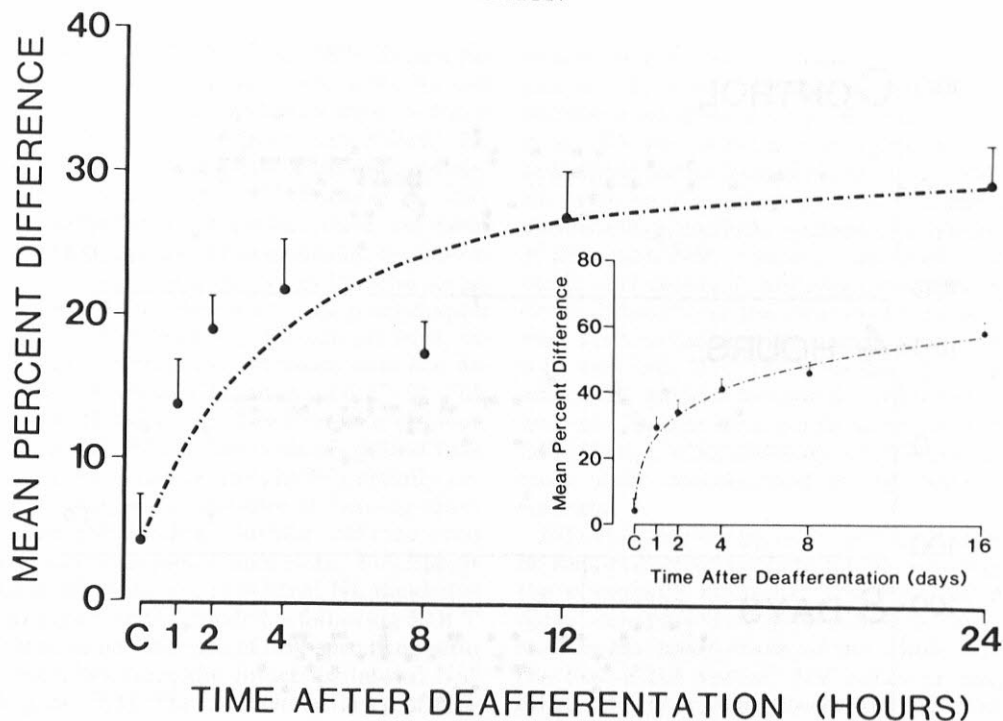


Fig. 9. The amount of ventral dendrite lost as a function of time after XDCT transection. The amount of dendrite lost for each cell is estimated by difference between the length of the dorsal dendrites (which predicts the normal ventral dendritic length) and the length of the atrophied ventral dendrites, taken as a percentage of the dorsal dendritic length. The mean of these ratios was computed for each survival time and for the control

population. Large graph: mean percent difference over the first 48 hours after deafferentation. Inset: mean percent difference as a function of days after surgery. Note that there is a very rapid loss such that the ventral dendrites are 14% shorter after 1 hour and 20% shorter after 2 hours. The atrophy continues at a slower rate throughout the 16-day interval examined.

gradual around 12 hours after the operation. The ventral dendrites continued to atrophy, resulting in a 60% difference in dendritic length at the longest time interval examined (16 days). This change in dendritic length with time is highly significant ($F(10,591) = 23.1, P < .0001$); the percent difference in dendritic length first became reliably different from the control value at 2 hours (least squares difference multiple range test, $P < .01$).

The "percent difference" value also was used to determine whether the atrophy of the ventral dendrites occurred uniformly across NL. Figure 10 shows the relationship between the percent difference (i.e., percentage of ventral dendrite lost) and the position of the cell for control animals and experimental animals surviving 4 hours and 8 days. The percentage of dendrite lost after deafferentation is completely independent of the location of the cell in the nucleus. For example, a cell in the anteromedial region of NL, which normally has short dendrites, will lose the same percentage of ventral dendritic length, as will a caudolateral cell with long dendrites after a similar survival time. The absolute amount of dendrite lost is, of course, much greater for the longer dendrites. In addition, if we assume that the dendrites are conical structures (no flat dendrites were observed), then the fact that the relationship between dendritic length and area remained constant (Fig. 2) necessarily means that the dendrites were becoming narrower (transversely) as they became shorter. These results were similar for the cells examined at each survival interval studied.

Number of primary dendrites

The loss of dendritic size observed in the present study could be effected in two ways: selectively, by the elimination of a few dendritic trees, or distributively, from throughout the dendrites. Since the number of primary dendrites on an NL cell also varies systematically as a function of position in the nucleus (Smith and Rubel, '79), the number of dendrites on the dorsal and ventral sides of each NL cell was examined by the same method as was dendritic length.

The number of dorsal and ventral primary dendrites per cell did not vary from control values and remained correlated ($0.55 < r < .75$) until 4 days after deafferentation. From 4 days to 16 days postsurgery the correlation dropped precipitously ($.10 < r < .45$); both the dorsal and ventral dendritic domains lost their gradients of dendritic number. In both cases, the changes were due to an increase in the number of primary dendrites on cells located in the middle to posterior sectors of the nucleus (where cells normally have few primary dendrites). Examination of these cells revealed that the increase in the number of primary dendrites was due to the appearance on the somata of very short ($< 10 \mu\text{m}$) processes on both sides of the cell body. In the animals surviving for 16 days, the "extra" processes on the ventral side of the cell were similar in length to the dendrites that had shrunken, and therefore may have resulted in an overestimation of the amount of "old" ventral

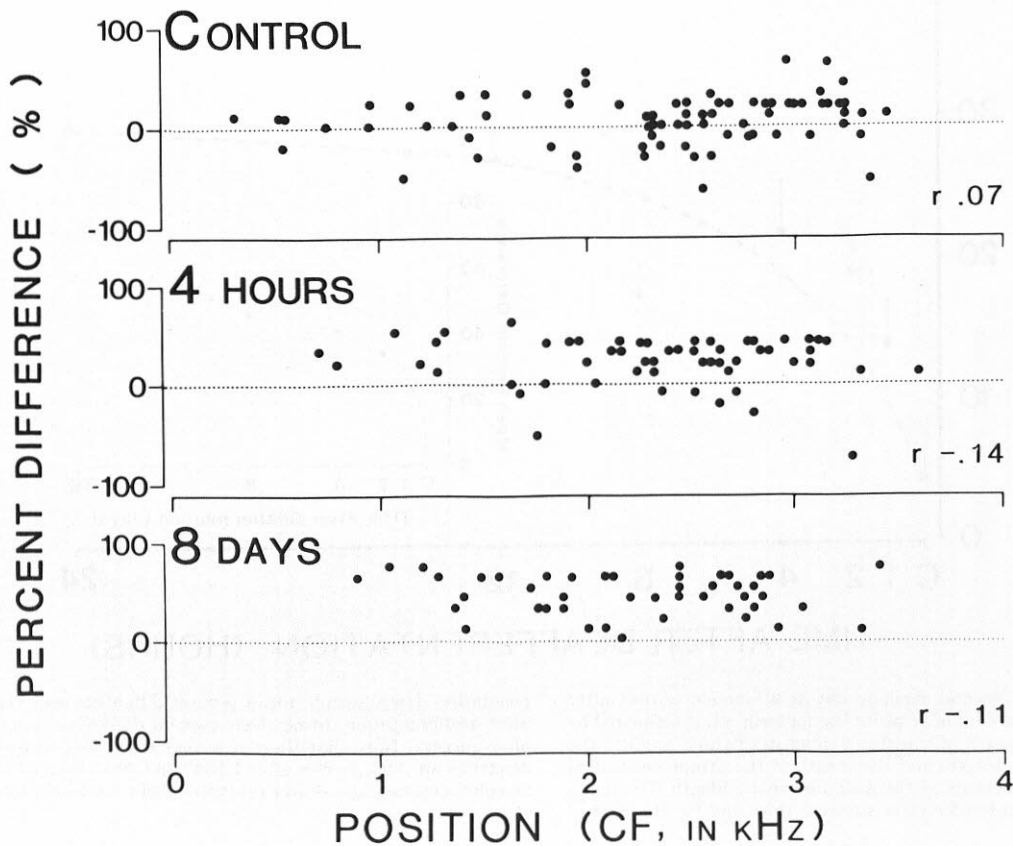


Fig. 10. Scatterplots showing the relationship between the position of an NL cell within the nucleus and the percent difference between its dorsal and ventral dendritic lengths: control cells, 4 hours after surgery, and 8

days after surgery. As there is no reliable correlation between these two parameters, the percentage of dendrite lost is independent of the position of the cell in the nucleus.

dendrite actually remaining. On the dorsal side, however, the addition of these processes did not increase the dendritic length beyond the normal range of variability.

The lack of an observable decrease in the number of ventral dendrites at short intervals after XDCT transection suggests that the manipulation is not resulting in the complete atrophy of only a selective few dendritic trees. Rather, the morphological changes appear to occur distributively throughout the dendritic domain.

DISCUSSION

The loss of the ventral dendrites after XDCT transection was first described by Benes et al. ('77) using an EM morphometric analysis of NL dendrites 4 days after XDCT transection. The volume density of dendrites in the ventral neuropil was found to be reduced by 85% compared to both the dorsal neuropil of the same animal and the ventral neuropil of control animals. Due to the differences in the breed, age, and sampling techniques used in this study and in that of Benes et al., the results from the two reports cannot be directly compared. Nevertheless, the change in dendritic length and concomitant change in dendritic diameter reported here would result in a decreased volume density of the ventral dendrites consistent with that reported by Benes et al. ('77).

Benes et al. ('77) also reported a decrease in the number of primary dendrites encountered (due to the decrease in cross-sectional area) and a general disruption of cytoplasmic organelles in the ventral portion of NL somata. No reliable changes in the size of the NL cell soma or nucleus, or in cell number, have been found at any time from 2 to 16 days postlesion (Rubel and Brandow, unpublished observations).

Time course of dendritic atrophy after deafferentation

Many previous investigations of postsynaptic changes following deafferentation do not report effects until days or weeks after the insult; others simply have not examined early time points (see Cowan, '70; Globus, '75). The results of this study, along with recent analyses of NM following cochlea removal (Born and Rubel, '84; Durham and Rubel, '84; Steward and Rubel, '84), show that events important for understanding the afferent axon-target neuron relationship occur much sooner than would be expected from previous studies. Several factors may account for the rapid morphological changes encountered in this study.

Transecting the XDCT removes a sizable amount of innervation from the ventral dendrites. Innervation from the contralateral NM accounts for at least 83% of the synapses

on the ventral NL dendrites (Parks et al., '83). Except for the infrequent ipsilateral NM axon that crosses the NL cell body lamina, it is the only known excitatory input to these dendrites (Rubel and Parks, '75; Parks and Rubel, '75; Jhaveri and Morest, '82). Investigations of the synaptology of NL suggest another input besides NM (Parks et al., '83), but its source or physiological properties have not been determined. In other examples of transneuronal degeneration, the manipulation removes a much smaller and sometimes unknown subset of the afferents to the postsynaptic surface. This partial deafferentation, in some systems, results in the sprouting of remaining afferents onto the denervated zone of the dendrite (Raisman and Field, '73; Parnavelas et al., '74; Rubel et al., '81; Hamill and Lenn, '83; Caceres and Steward, '83). It has been suggested that the lack of a severe transsynaptic atrophy of partially denervated dendrites is due to the presence of "saving afferents," which maintain the dendritic surface and may even take over the abandoned synapses (Rubel et al., '81). Apparently the remaining afferents to the ventral NL dendrites are not sufficient to maintain the dendrites following XDCT transection, and there is no evidence of any sprouting onto the deafferented dendrites from the intact ipsilateral NM projection (Rubel et al., '81). The relative severity of this manipulation, in other words, may account for the unusual rapidity of the dendritic reaction.

The dendritic changes in NL may also be more rapid than those seen in other systems due to the proximity of the lesion to the terminals. Transection of the XDCT at the midline leaves an axon stump on the order of 0.5–1.5 mm in length still connected to the ventral dendrites. This is considerably shorter than the stump left in other preparations used to study deafferentation, i.e., eye enucleation, dorsal column lesion, olfactory epithelia ablation, and peripheral nerve section. The time course of changes in muscle membrane properties after motor nerve section can be altered by varying the length of the distal nerve stump (see Rosenthal, '77). Although transport may continue in the NM axon distal to the lesion (Young and Rubel, '83), the time course of changes in release of substances from the NM terminals is not known.

On the other hand, the time course of changes in synaptic activity is known. We have made extracellular electrophysiological recordings from the dorsal and ventral NL neuropils during XDCT transection (Deitch and Rubel, unpublished observations). In all cases there was an immediate cessation of the normally high levels of both acoustically driven and spontaneous activity in the ventral neuropil, while both spontaneous and driven activity remained normal in the dorsal neuropil. Thus, the rapid onset of dendritic atrophy in ventral NL is preceded by the immediate cessation of action potentials.

Localization of atrophy to the deafferented surface

Another significant facet of these results is the restriction of the changes in dendritic size to the deafferented surface. Sectioning of the NM axon collaterals crossing the midline does not evoke any obvious degenerative changes in NM cell bodies and presumably does not damage the branch of the NM axons that innervates the dorsal NL dendrites (Parks and Rubel, '75; Rubel et al., '81). It is assumed that the postsynaptic surface of the dorsal dendrites was main-

tained because these synapses continued to be active. Localized dendritic alterations also occur on cricket interneurons after unilateral cercal extirpation (Murphey et al., '75) and on rat dentate gyrus granule cells following entorhinal cortex lesions (Caceres and Steward, '83). In the cat brain stem auditory system, unilateral ablation of the anteroventral cochlear nucleus (the mammalian homologue of the avian NM) results in the preferential shrinkage of the lateral neuropil (ipsilaterally) and the medial neuropil (contralaterally) of the neurons in the medial superior olivary nucleus (apparently homologous to NL) after 2 weeks (Liu and Liu, '71). The neuropil opposite the denervated side of the nucleus remained similar to that seen in control animals. Earlier time points were not reported. The regulatory action of an afferent on its target neuron is therefore most likely concentrated at the postsynaptic surface it contacts.

Afferents remaining after partial deafferentation would be required to compensate for the lost regulatory action of the eliminated afferents. The eventual alteration of the dorsal dendrites (i.e., spine formation) may be a result of a shift in the homeostasis of the whole cell after "sensing" the loss of the ventral NM axons or may be induced by other afferent axons. Sotelo and Arsenio-Nunes ('76) described the appearance of spines on the normally smooth Purkinje cell proximal dendritic branches after neonatal climbing fiber destruction. Angaut et al. ('82) determined that the new spines are postsynaptic to parallel fibers which do not normally innervate that dendritic region. The possibility of a new input to the dorsal NL dendrites has not been carefully examined.

It is also of interest to note that the *percentage* of dendrite lost, rather than the absolute length, is consistent throughout the nucleus at each survival time. Thus, the amount of dendrite lost at any time is proportional to the amount of dendrite available. Since the density of synapses on the NL dendrites is constant throughout the nucleus (Parks et al., '83), the degree of dendritic atrophy is proportional to the degree of innervation lost, again suggesting local control of the postsynaptic surface.

Cellular events during transneuronal atrophy

The results of this study set some constraints on hypotheses of the cellular reaction to deafferentation. In order to attain such a rapid loss of dendrite by resorption (rather than a breaking off), several physical barriers must be overcome. For one, either the synapse must become uncoupled, or the degenerating terminal must be dragged along by the withdrawing dendrite. Benes et al. ('77) noted a large decrease in the number of boutons contacting the dendrites and astrocytic processes inserted between the remaining pre- and postsynaptic membranes. A similar result was reported by Gentschev and Sotelo ('73) in the cochlear nucleus within 24 hours after cochlear removal. On the other hand, Wisniewski et al. ('72) found heavily degenerated terminals still opposed to postsynaptic densities 12 days after deafferentation of monkey lateral geniculate nucleus. After degeneration of the terminals, examples also have been found of dendrites phagocytosing the degenerating terminal (Walberg, '63; Hamill and Lenn, '83) and of glia engulfing a portion of the dendrite along with the degenerating terminal (Ghetti et al., '75).

A second physical restraint imposed by the unchanging size of the cell soma and dorsal dendrites is the disposal of membrane. Although not described yet in neurons, an increase in the rate of formation and size of endocytotic vesicles has been reported in deafferented muscle cells (Libelius et al., '78). The present results support the idea that afferent regulation of the rate of addition and/or removal of membrane must be limited to the specific target surface, since the same amount of membrane is still maintained on the dorsal dendrites and on the soma.

Third, in order to resorb an entire dendrite, especially to the degree found 16 days after XDCT transection, the intradendritic structure (cytoskeleton, endoplasmic reticulum) must be dismantled. Ghetti et al. ('75), LeVay ('71), and Benes et al. ('77) have reported examples of "washed out" dendrites (lacking microtubules and organelles) opposed to degenerating terminals. In addition, Solomon ('80) has demonstrated the resorption of neuroblastoma neurites within an hour after microtubule disassembly is induced. Thus, afferent regulation of the cytoskeleton and of transport functions in the target dendrites is also consistent with the time course of changes seen in the present study.

Finally, the results of the present study may offer insight into the normal processes regulating dendritic form. It will be of considerable importance to determine what properties of dendritic form are controlled by intracellular factors, such as the genome, as opposed to extracellular factors, such as where the cell resides in relation to other cells and the pattern of innervation and activation it receives. This is especially important in understanding the highly regular arrangement of dendritic fields such as found in NL. The fact that the absolute size of the ventral dendrites decreases throughout the nucleus implies a major role for the afferent in regulating dendritic size. That the gradient of dendritic size also disappears in the ventral neuropil strongly suggests that the pattern of afferent innervation determines the dendritic architecture of the nucleus as a whole.

ACKNOWLEDGMENTS

We greatly appreciate the efforts of Zaid Smith in the collection of data and for his suggestions on the Golgi method. We also thank Lincoln Gray for his advice on the statistical analyses, Elizabeth Cantrell for her excellent assistance with the artwork, and Don Born, Dianne Durham, Sally Moody, and Nicholas Lenn for their helpful suggestions on the manuscript. This research was supported by NIH grant # NS 15395 and RCDA # NS 00305 (E.W.R.), the Lions of Virginia Hearing Foundation, and the University of Virginia Pratt Foundation.

LITERATURE CITED

- Angaut, P., R.M. Alvarado-Mallart, and C. Sotelo (1982) Ultrastructural evidence for compensatory sprouting of climbing and mossy afferents to the cerebellar hemisphere after ipsilateral pedunculotomy in the newborn rat. *J. Comp. Neurol.* 205:101-111.
- Bernstein, J.J., and N.A. Standler (1983) Dendritic alteration of rat spinal motoneurons after dorsal horn mince: Computer reconstruction of dendritic fields. *Exp. Neurol.* 82:532-540.
- Benes, F.M., T.N. Parks and E.W. Rubel (1977) Rapid dendritic atrophy following deafferentation: An EM morphometric analysis. *Brain Res.* 122: 1-13.
- Born, D.E., and E. W. Rubel (1984) Afferent influences on brain stem auditory nuclei of the chicken: Neuron number and size following cochlea removal. *J. Comp. Neurol.* (in press).
- Boord, R.L. (1969) The anatomy of the avian auditory system. *Ann. N.Y. Acad. Sci.* 167:186-198.
- Caceres, A., and O. Steward (1983) Dendritic reorganization in the denervated dentate gyrus of the rat following entorhinal cortical lesions: A golgi and electron microscopic analysis. *J. Comp. Neurol.* 214:387-403.
- Cowan, W.M. (1970) Anterograde and retrograde transneuronal degeneration in the central and peripheral nervous system. In W.J. H. Nauta and S.O.E. Ebbesson (eds): *Contemporary Research Methods in Neuroanatomy*. New York: Springer-Verlag, pp. 217-249.
- Deitch, J.S., and E.W. Rubel (1982) Time course of changes in dendritic morphology in n. laminaris following deafferentation. *Soc. Neurosci. Abstr.* 8:756.
- Durham, D. (1982) *Anatomical and Functional Plasticity in the Developing Mouse Central Trigeminal Pathway*. Doctoral dissertation, Washington University, St. Louis.
- Durham, D., and E.W. Rubel (1984) Afferent influences on brain stem auditory nuclei of the chicken: Changes in succinate dehydrogenase activity following cochlea removal. *J. Comp. Neurol.* (in press).
- Durham, D., and T.A. Woolsey (1984) Effects of neonatal whisker lesions on mouse central trigeminal pathways. *J. Comp. Neurol.* 223:424-447.
- Gentschev, T., and C. Sotelo (1973) Degenerative patterns in the ventral cochlear nucleus of the rat after primary deafferentation: An ultrastructural study. *Brain Res.* 62:37-60.
- Ghetti, B., D.S. Horoupian, and H.M. Wisniewski (1975) Acute and long-term transneuronal response of dendrites of lateral geniculate neurons following transection of the primary visual afferent pathway. *Adv. Neurol.* 12:401-424.
- Globus, A. (1975) Brain morphology as a function of presynaptic morphology and activity. In A.H. Riesen (ed): *The Developmental Neuropsychology of Sensory Deprivation*. New York: Academic Press, pp. 9-91.
- Grant, G. (1970) Neuronal changes central to the site of axon transection: A method for the identification of retrograde changes in perikarya, dendrites and axons by silver impregnation. In W.J.H. Nauta and S.O.E. Ebbesson (eds). *Contemporary Research Methods in Neuroanatomy*. New York: Springer-Verlag, pp. 173-185.
- Gray, L., Z. Smith, and E.W. Rubel (1982) Developmental and experiential changes in dendritic symmetry in n. laminaris of the chick. *Brain Res.* 244:360-364.
- Gulley, R.L., R.J. Wenthold, and G.R. Neises (1977) Remodeling of neuronal membranes as an early response to deafferentation. A freeze-fracture study. *J. Cell Biol.* 75:837-850.
- Hackett, J.T., H. Jackson, and E.W. Rubel (1982) Synaptic excitation of the second and third order auditory neurons in the avian brain stem. *Neuroscience* 7:1455-1469.
- Hamill, G.S., and N.J. Lenn (1983) Synaptic plasticity within the interpeduncular nucleus after unilateral lesions of the habenula in neonatal rats. *J. Neurosci.* 3:2128-2145.
- Jhaveri, S., and D.K. Mores (1982) Neuronal architecture in nucleus magnocellularis of the chicken auditory system with observations on nucleus laminaris: A light and electron microscopic study. *Neuroscience* 7:809-836.
- Jones, W.H., and D.B. Thomas (1962) Changes in the dendritic organization of neurons in the cerebral cortex following deafferentation. *J. Anat.* 96:375-381.
- Kupfer, C., and J.L. deC. Downer (1967) Ribonucleic acid content and metabolic activity of lateral geniculate nucleus in monkey following afferent denervation. *J. Neurochem.* 14:257-263.
- LeVay, S. (1971) On the neurons and synapses of the lateral geniculate nucleus of the monkey, and the effects of eye enucleation. *Z. Zellforsch. Mikros. Anat.* 113:396-419.
- Libelius, R., I. Lundquist, W. Templeton, and S. Thesleff (1978) Intracellular uptake and degradation of extracellular tracers in mouse skeletal muscle *in vitro*: The effect of denervation. *Neuroscience* 3:641-647.
- Lippe, W.R., O. Steward, and E.W. Rubel (1980) The effect of unilateral basilar papilla removal upon nuclei laminaris and magnocellularis of the chick examined with [³H]2-deoxy-D-glucose autoradiography. *Brain Res.* 196:43-58.
- Liu, C.N., and C.Y. Liu (1971) Role of afferents in maintenance of dendritic morphology. *Anat. Rec.* 169:369(abstract).
- Meyer, M.R., and J.S. Edwards (1982) Metabolic changes in deafferented central neurons of an insect, *Acheta domesticus*. I. Effects upon amino acid uptake and incorporation. *J. Neurosci.* 2:1651-1659.
- Murphey, R.K., B. Mendenhall, J. Palka, and J.S. Edwards (1975) Deafferentation slows the growth of specific dendrites of identified giant interneurons. *J. Comp. Neurol.* 159:407-418.
- Parks, T.N. (1979) Afferent influences on the development of the brain stem

- auditory nuclei of the chicken: Otocyst ablation. *J. Comp. Neurol.* 183:665-678.
- Parks, T.N. (1981) Changes in the length and organization of nucleus laminaris dendrites after unilateral otocyst ablation in chick embryos. *J. Comp. Neurol.* 202:47-57.
- Parks, T.N., P. Collins, and J.W. Conlee (1983) Morphology and origin of axonal endings in nucleus laminaris of the chicken. *J. Comp. Neurol.* 214:32-42.
- Parks, T.N., and E.W. Rubel (1975) Organization and development of brain stem auditory nuclei of the chicken: Organization of projections from n. magnocellularis to n. laminaris. *J. Comp. Neurol.* 164:435-448.
- Parnavelas, J.G., G. Lynch, N. Brecha, C.W. Cotman, and A. Globus (1974) Spine loss and regrowth in hippocampus following deafferentation. *Nature* 248:71-73.
- Pinching, A.J., and T.P.S. Powell (1971) Ultrastructural features of trans-neuronal cell degeneration in the olfactory system. *J. Cell Sci.* 8:253-287.
- Raisman, G., and P.M. Field (1973) A quantitative investigation of the development of collateral reinnervation after partial deafferentation of the septal nuclei. *Brain Res.* 50:241-264.
- Ramón y Cajal, S. (1908) Les ganglions terminaux du nerf acoustique des oiseaux. *Trab. Inst. Cajal Invest. Biol.* 6:195-225.
- Rosenthal, J. (1977) Trophic interactions of neurons. In E.R. Kandel (ed): *Handbook of Physiology*, Sec. 1, Vol. 1. Bethesda: Am. Physiol. Soc., pp. 775-801.
- Rubel, E.W., and T.N. Parks (1975) Organization and development of brain stem auditory nuclei of the chicken: Tonotopic organization of n. magnocellularis and n. laminaris. *J. Comp. Neurol.* 164:411-434.
- Rubel, E.W., and Z.D.J. Smith (1981) Afferent maintenance of dendritic organization in n. laminaris of the chick. *Anat. Rec.* 199:219A(abstract).
- Rubel E.W., Z.D.J. Smith, and O. Steward (1981) Sprouting in the avian brain stem auditory pathway: Dependence on dendritic integrity. *J. Comp. Neurol.* 202:397-414.
- Ruiz-Marcos, A., and F. Valverde (1970) Dynamic architecture of the visual cortex. *Brain Res.* 19:25-39.
- Smith, D.E. (1974) The effect of deafferentation on the postnatal development of Clarke's nucleus in the kitten—A golgi study. *Brain Res.* 74:119-130.
- Smith, D.J., and E.W. Rubel (1979) Organization and development of brain stem auditory nuclei of the chicken: Dendritic gradients in nucleus laminaris. *J. Comp. Neurol.* 186:213-240.
- Smith, Z.D.J. (1981) Organization and development of brain stem auditory nuclei of the chicken: Dendritic development in n. laminaris. *J. Comp. Neurol.* 203:309-333.
- Solomon, F. (1980) Neuroblastoma cells recapitulate their detailed neurite morphologies after reversible microtubule disassembly. *Cell* 21:333-338.
- Sotelo, C., and M.L. Arsenio-Nunes (1976) Development of Purkinje cells in absence of climbing fibers. *Brain Res.* 111:389-395.
- Stensaas, L.J. (1967) The development of hippocampal and dorsolateral pallial regions of the cerebral hemisphere in fetal rabbits. I. Fifteen millimeter stage, spongioblast morphology. *J. Comp. Neurol.* 129:59-70.
- Steward, O., and E.W. Rubel (1984) Afferent influences on brain stem auditory nuclei of the chicken: Cessation of protein synthesis as an antecedent to age dependent transneuronal degeneration. *J. Comp. Neurol.* (submitted).
- Valverde, F. (1968) Structural changes in the area striata of the mouse after enucleation. *Exp. Brain Res.* 5:274-292.
- Walberg, F. (1963) Role of normal dendrites in removal of degenerating terminal boutons. *Exp. Neurol.* 8:112-124.
- White, L.E., Jr. and L.E. Westrum (1964) Dendritic spine changes in prepyriform cortex following olfactory bulb lesions—rat, Golgi method. *Anat. Rec.* 148:410-411.
- Wisniewski, H.M., B. Ghetti, and D.S. Horoupian (1972) The fate of synaptic membranes of degenerating optic nerve terminals and their role in the mechanism of trans-synaptic changes. *J. Neurocytol.* 1:297-310.
- Young, S.R., and E.W. Rubel (1983) Frequency specific projections of single auditory neurons. *J. Neurosci.* 3:1373-1378.